



Synthesis and Optimization of Anodic Aluminium Oxide Thin Film Electrode for DNA Sensing

by

**Shahidah Arina Shamsuddin
(1541911717)**

A thesis submitted in fulfillment of the requirements for the degree of
Doctor of Philosophy

**Institute of Nano Electronic Engineering
UNIVERSITI MALAYSIA PERLIS**

2021

ACKNOWLEDGEMENT

Alhamdulillah, praised to Allah, who has given me the opportunity, health and strength to complete my study. My first gratitude and deepest respect goes to my main supervisor, P.M Dr. Mohd. Nazree bin Derman, for his commitment, helps, encouragement and guidance during completing my research. Thank you for your support for whole this time. You never push me out of my limit. You always understand my situation. You always trust and give me freedom to explore everything that I wanted to learn. Thank you so much for your faith on me. There is not enough words to describe how much I appreciate on how you train me until I become as who I am today.

Special thanks to my co-supervisor, Prof. Dr. Uda Hashim, for his encourage ideas, motivation, and valuable advice, as long as the lab facilities were being provided for the whole research which helped me to finish this study. Special appreciation goes to Dr Nur Hamidah and Dr. Nuzaihan for their helps and guidance in submitting these theses. Next, I would like to express my gratitude to INEE technicians and teaching engineers, Ms. Nor Shamyra, Mr. Loqman, Mr. Jasni and Mr. Isa, who have provided laboratory help support for whole this years. A special memory goes to our late technician, Mr Aizat who has leaved us with a golden time to be remembered. You are such a very kind person. I am pretty sure your baby, little cute Ana will be always protected and love by Allah.

Special thanks goes to my lecturers, Dr Faris, Dr Azizah, and Dr Gopinath for their helps in the laboratory, guidance and changing knowledge. To my all beloved cuddly friends, I love you guys so much, Dr Conlathan, Syifa, Lala, Thivina, Khai, Santhraleka, Ishwary, Indra, Afnan, Aiman, Tikah, Iman, Adelyn, Lam, Azrul, Fatin, Mr Steven and of course Adila. Thank you for loving me as your friend, staying up over the night for completing this thesis. And of course thank you so much for helping me taking care of my little baby, Afina. I will definitely make sure she remembers you guys even after she's grown up. I will never forget all the joy, laughs and tears with you guys. Also not to forget, Adzhari, Huda, Lee, Suhaimi, Tony, Zaki, Muaz, Nazawa, Humaira, Farah, Dr Sharifah, Dr Siti, Suhaily, Dr Zen, Dr Lon, Haq, and Nor Syamimi. Thank you for being my great companions for all this time. I truly enjoyed and appreciated the moments shared with you guys back then. Special appreciation from the bottom of my heart to Dr Conlathan, Mr Jasni and Miss Atiqah, Dr Syikin, Dr Afiqah, and Thivina, who had help me in proofreading, editing, paraphrasing, and even consulting to upgrade my thesis prior to submission. Thank you so much. Very much appreciate it.

Special appreciation goes to my parents, Mdm Rominah Paimon and Mr Shamsuddin @ Cikgu Chodets, who have sacrificed a lot for me. Mak abah, this glory is for you. With your doa and love, I've made it. There are not enough words to say how much I love you guys. I want you to know that I love and miss you always. You have always supported and believed in me. You guys never clip my wings. You let me decide my own decision in everything I do since I was in school until now. You even let me choose my man. He is the best husband ever for me. To my husband, Mr Faheem, you are my perfect ten. I am always proud of you. You keep on cheers me up with your stupid jokes. You are the kindest heart, hardworking, loving and caring person. I always appreciate your existence in my life as my other half. I am really thankful to have you in my life. I love you so much to the moon and back. Thank you so much for always being there for me and taking care of our child while letting me finish all this things. To my adorable little girl Nur Afina Safiya, thank you for bring all the joy, laughter, love and happiness in our life. We all love you so much. You are the cutest and funniest little kid ever. Finally, deepest love to all my family members, my in-law, Mdm Rohani and Mr Tahir, my siblings, Sharifah and Nurrobby, for all their continuously support and love that they gave me. Thank you all.

TABLE OF CONTENTS

	PAGE
DECLARATION OF THESIS	i
ACKNOWLEDGEMENT	ii
TABLE OF CONTENTS	iii
LIST OF TABLES	vii
LIST OF FIGURES	ix
LIST OF ABBREVIATIONS	xv
LIST OF SYMBOLS	xvii
ABSTRAK	xix
ABSTRACT	xxi
CHAPTER 1 : INTRODUCTION	1
1.1 Background	1
1.2 Problem Statement	5
1.3 Research Objective	8
1.4 Research Scopes	9
1.5 Thesis Outline	11
CHAPTER 2 : LITERATURE REVIEW	13
2.1 Anodization Process of Aluminium Substrate	13
2.2 Theory on the Growth Formation of Anodic Aluminium Oxide	17
2.3 Self-Organisation of Porous AAO	24
2.4 Single-Step Anodizing Method for Synthesizing the AAO Porous Structure	26

2.5	The Applications of Anodic Aluminium Oxide in Chemical and Biological Sensing Detections	33
2.6	Nanoporous Based-DNA Biosensor	39
2.6.1	Types of Nanoporous Based-DNA Biosensor and Their Performance	39
2.6.2	Nanoporous Materials: Synthesis Methods, Geometrical Differences, Superiority and Limitations.	45
2.6.3	Impedimetric Properties of the AAO-DNA Based Biosensor	55
2.7	Surface chemical studies of anodic aluminium oxide (AAO)	64
2.8	Design of Experiments (DOE) Versus Taguchi Method	69
2.9	The Basic Principle of Taguchi Experimental Design.	72
2.10	Optimization Method Used for Optimizing the Anodizing Parameters	76
CHAPTER 3 : METHODOLOGY		79
3.1	Preparation of Aluminium Thin Films Electrodes	81
3.2	Anodization Process	82
3.3	AAO Surface Characterization Procedure	85
3.3.1	Morphological Observation	85
3.3.2	Structural (XRD) and Surface Functionality Analysis (FTIR)	86
3.4	Electrochemical Test Procedures	87
3.5	Surface Modification, Immobilization and Hybridization of DNA	88
3.6	Sensitivity, Limit of Detection (LOD) and Selectivity Test	92
3.7	Optimization of Anodizing Parameters	93
3.7.1	Step 1: Identifying the Main Function, Side Effects, and Failure Modes	95
3.7.2	Step 2: Identifying Noise Factors and Testing Conditions for Evaluating Quality Loss	97
3.7.3	Step 3: Identifying Quality Characteristic and Objective Function	99
3.7.4	Step 4: Identifying the Alternate Levels for Each Control Factor	102
3.7.5	Step 5: Selecting an Orthogonal Array Matrix for the Experiments	104

3.7.6	Step 6: Conducting the Experiments	106
3.7.7	Step 7: Analysing the Data	107
3.7.8	Step 8: Conducting a Verification or Confirmation Experiment and Planning for Future Action	109
CHAPTER 4 : RESULTS & DISCUSSION		111
4.1	Evaluation of AAO Growth Mechanism	111
4.2	AAO Pore Widening Observations by Time	115
4.3	Surface Characterization of Anodic Aluminium Oxide (AAO)	121
4.3.1	Crystallinity Characterization	121
4.3.2	Surface Functionalities Characterization	123
4.4	Study on the Effects of Anodizing Parameters on the Changes of AAO Pores Dimensional Properties	126
4.4.1	Effects of the Anodizing Voltage on AAO Pore Dimensional Properties	126
4.4.2	Effects of the Anodizing Temperature on AAO Pores Dimensional Properties	132
4.4.3	Effects of the Anodizing Time on AAO Pores Dimensional Properties	137
4.4.4	Effects of Electrolyte Concentration to the AAO Pores Dimensional Properties	142
4.5	Influence of AAO Pore Dimensional Properties on its Electrical Performance in Detecting DNA Hybridization	148
4.5.1	Electrocatalytic Mechanism of Anionic Ferricyanide Ions at the AAO-Modified Electrode Surfaces	148
4.5.2	Influence of AAO Pore Dimensional Properties on the Resistance Charged Transfer (R_{ct})	158
4.5.3	Influence of AAO Pore Dimensional Properties on the AAO Thin Film Electrode-Based DNA Biosensor Sensitivity Performance	163
4.6	Optimization of AAO Anodizing Parameters using L9 Taguchi Orthogonal Arrays	168

4.6.1	Optimization of the AAO Anodizing Parameters at the Optimum Levels for Sensitivity and Limit of Detection (LOD)	169
4.6.2	Percentage Influence of Anodizing Parameters on the Detection Sensitivity and Limit of Detection (LOD)	173
4.7	Repetition Experiments to Test the Effectiveness of Taguchi Optimization Method in Optimizing the AAO Anodizing Parameters	180
4.7.1	Morphological Observation	180
4.7.2	Sensitivity Test and Limit of Detection (LOD)	182
4.7.3	Selectivity Test	187
CHAPTER 5 : CONCLUSIONS AND FUTURE WORK		191
5.1	Conclusions	191
5.2	Recommendations for Future Work	193
REFERENCES		196
APPENDIX A FORMULA AND CALCULATION		210
APPENDIX B ADDITIONAL DATA ON THE EFFECTS OF ANODIZING PARAMETERS TO AAO THIN FILM ELECTRODE DIMENSIONAL PROPERTIES		213
APPENDIX C ADDITIONAL DATA ON THE INFLUENCED OF AAO DIMENSIONAL PROPERTIES ON THE CHARGE TRANSFER RESISTANCE (R_{CT})		215
APPENDIX D ADDITIONAL DATA ON THE INFLUENCED OF AAO DIMENSIONAL PROPERTIES ON THE AAO THIN FILM ELECTRODE-BASED DNA BIOSENSOR SENSITIVITY PERFORMANCE		216
APPENDIX E NYQUIST PLOTS, SENSITIVITY AND LIMIT OF DETECTION CALCULATIONS FOR TAGUCHI OPTIMIZATION EXPERIMENTAL SAMPLES		220
LIST OF PUBLICATIONS		233

LIST OF TABLES

	PAGE
Table 2.1 Nanoporous based DNA biosensor synthesized by different materials and methods.	41
Table 2.2 Advantages and disadvantages of different Au nanoporous fabrication techniques (Bhattacharai et al., 2018).	46
Table 2.3 Fitting data of equivalent circuits for (A) Al foil, (B) first step anodization AAO, (C) AAO after etched, and (D) second step anodization AAO (Wang et. al., 2014).	57
Table 2.4 Fitting parameters of equivalent circuits (Takmakov, P., et. al., 2006)	59
Table 2.5 Comparison of the fitting data analysed for PNA- modified and PNA/DNA-modified nanoporous gold electrodes (Tao W. et. al., 2017)	62
Table 2.6 Fitting data parameter of the platinum-AAO membrane (Deng, J., & Toh, C. S., 2013).	62
Table 2.7 Taguchi Orthogonal Arrays selector (Davis, R., & John, P., 2018).	74
Table 3.1 Single-step anodization at different anodizing parameters conditions.	84
Table 3.2 Information on the sequences of the probe and target DNA.	91
Table 3.3 Noise factors of an experiment.	99
Table 3.4 Control factors and their levels.	103
Table 3.5 L9 Taguchi Orthogonal Arrays.	106

Table 4.1	The effects of pores size and porous thickness on the charged transfer resistance (R_{ct}).	158
Table 4.2	Effects of pores size, AAO thickness and surface area on the sensitivity of AAO thin film electrodes to detect DNA hybridization event.	164
Table 4.3	The output response and the values of SNR (η).	171
Table 4.4	Average of η by factor levels (dB)	171
Table 4.5	Dimensional properties of optimized AAO thin film electrode.	181
Table 4.6	Percentage improvements.	185

©This item is protected by original copyright

LIST OF FIGURES

	PAGE
Figure 1.1	Illustration of the basic biosensor system. 2
Figure 2.1	Schematic diagrams of the AAO stages formation (a-d) and current density versus time transient of the AAO grown at constant voltage (C. Cheng & Ngan, 2015). 14
Figure 2.2	Electrochemical reactions involved in the formation of the basic aluminum oxide barrier layer during the anodization process in an acidic solution (Chi Lu & Zhi Chen, 2011). 17
Figure 2.3	Mechanism of the pore formation initiated by the field-effect-assisted dissolution (O'Sullivan & Wood, 1970). 20
Figure 2.4	Field effect assisted dissolution during the AAO growth formation (a) before polarization, (b) after polarization, (c) the removal of Al^{3+} and O^{2-} ions, and (d) the remaining oxide (O'Sullivan & Wood, 1970). 21
Figure 2.5	SEM and FFT (Fast Fourier Transform) images of AAO anodized with single-step anodizing method: (a) before and (b) after etching with the mixture of chromic and phosphoric acid solution (C H Voon, Derman, Hashim, Ahmad, & Ho, 2014). 26
Figure 2.6	SEM images of AAO film grown by (a) single-step and (b) two-step of anodizing method at 45 V in 0 °C of 0.5 M oxalic acid for 48 hours (Yang et al., 2007). 29
Figure 2.7	Cross section images of the AAO film grown by the single-step anodization at (a) 800x and (b) 20kx of magnification under SEM observation (Yang et al., 2007). 30

Figure 2.8	SEM images of the AAO film grown by single-step anodization at 60 V in 0.3 M of oxalic acid at (a) 20 °C, (b) 30 °C and (c) 40 °C for 1 hour. (Bruera et al., 2019).	32
Figure 2.9	(a) AAO dimensional properties: pore diameter (D_p), interpore distance (D_{int}), pore length (L_p), pore wall thickness (τ_w) and oxide barrier thickness (τ_{obl}). (b) SEM images of top and cross-section views of AAO (Santos et al., 2013).	34
Figure 2.10	FESEM images of nanoporous gold fabricated by dealloying process in $ZnCl_2$ and benzyl alcohol at 120 °C (Jia, Yu, Ai, & Zhang, 2007).	47
Figure 2.11	3D reconstructed TEM tomography image showing the internal structure of nanoporous gold (Fujita, Qian, Inoke, Erlebacher, & Chen, 2008).	47
Figure 2.12	SEM images at (a) top view and (b) cross sectional (after been PVD evaporated with gold), of porous Si anodic etched in 4% HF in dimethylformamide solution, at 7.7 mA/cm ² of current density (Kleps et al., 2009).	49
Figure 2.13	SEM images of SnO ₂ films deposited onto ITO substrate at -1.0 V (vs. Ag/AgCl) with charge density (Q) of 0.8 C·cm ⁻² (Le et al., 2015).	51
Figure 2.14	FESEM images of Nb ₂ O ₅ nanoporous film which synthesized by the anodization method in 1 wt.% HF+1M H ₃ PO ₄ at 2.5V (vs. Ag/AgCl, 3M KCl) for 1 hour : (a) top and (b) cross-sectional view.	52
Figure 2.15	FESEM images of (a) top and (b) cross sectional view of AAO nanoporous grown by anodization in 0.3 M oxalic acid at 10 °C and 45 V.	54
Figure 2.16	Morphologies after different stages of two-step anodization, showing (a) the scratches on Al foil surface, (b) surface of	

	specimen after the first step anodization, (c) Al substrate after surface etched, and (d) surface of specimen after the second step anodization (Wang J. Z., et. al., 2014).	56
Figure 2.17	FESEM images of nanoporous gold electrode at $\times 80000$ magnification (Tao W. et. al., 2017).	61
Figure 2.18	X-ray photoelectron spectrum of the two-step AAO (Ilango et al., 2016).	64
Figure 2.19	Individual x-ray photoelectron spectra of the two-step AAO: (a) Al 2p, (b) O 1s and (c) C 1s (Ilango et al., 2016).	65
Figure 2.20	XPS spectra of the AAO membranes anodized in different type of electrolytes. (a) Phosphoric acid (b) Oxalic/phosphoric acid mixture and (c) Oxalic acid (Treverton, J. A., et. al., 1993).	67
Figure 2.21	C 1s peaks in XPS spectra of asymmetric layers of AAO membranes (Treverton, J. A., et. al., 1993).	68
Figure 3.1	Flow chart of the research methodology.	80
Figure 3.2	Anodizing process set up.	82
Figure 3.3	Illustration of AAO surface modification steps that involved the silanization process by APTES, activation with glutaraldehyde, immobilization of aminated ssDNA probe and finally the hybridization of the ssDNA target.	89
Figure 3.4	Illustration of AAO surface modification steps silazation process by APTES, activation of glutaraldehyde, immobilization of aminated ssDNA probe and finally the hybridization of the ssDNA target.	89
Figure 3.5	Steps for conducting Taguchi robust design experiments.	94

Figure 4.1	Study on the electrical response of anodization process of AAO thin film electrode. (a) Current density versus time gradient graph of Al thin film anodized at 40V in 0.3 M oxalic acid. (b) Illustration of AAO nanoporous formation stages.	112
Figure 4.2	FESEM images of AAO thin film electrode post-etching in 5 % H_3PO_4 at 30 °C for (a) 0 minute, (b) 10 minutes, (c) 20 minutes and (d) 30 minutes. Inset images show the FFT (Fast Fourier Transform) images analysis for each FESEM image.	116
Figure 4.3	Cross-sectional AAO morphology on the growth process under constant voltage reported by Cheng & Ngan (2015).	119
Figure 4.4	XRD patterns of AAO anodized at 40 V in 0.3 M of oxalic acid at 15 °C for 60 minutes.	121
Figure 4.5	IR spectra of AAO after anodized in oxalic acid.	124
Figure 4.6	FESEM top view images of AAO thin film electrodes at different anodizing voltages.	127
Figure 4.7	Correlation graphs of AAO dimensional properties versus anodizing voltage anodized in 0.3 M oxalic acid at 15 °C for 1 hour.	129
Figure 4.8	Schematic illustration of Joule heating dissipation that occurs during the anodization process at (A) <30 V and (B) >30 V	130
Figure 4.9	FESEM top view images of AAO thin film electrodes at different anodizing temperatures.	133
Figure 4.10	Correlation graphs of AAO dimensional properties versus anodizing temperature, which anodized in 0.3 M oxalic acid at 40 V for 1 hour.	135
Figure 4.11	FESEM top view images of AAO thin film electrodes at different anodizing times.	138

Figure 4.12	Correlation graphs of AAO dimensional properties versus anodizing time, which anodized in 0.3 M oxalic acid at 15 °C and 40 V for 30 to 90 minutes.	140
Figure 4.13	FESEM top view images of AAO thin film electrodes at different electrolyte concentrations.	143
Figure 4.14	Correlation graphs of AAO pores dimensional properties versus electrolyte concentration, anodized at 15 °C and 30 V for about 1 hour.	144
Figure 4.15	EIS measurement mechanism of bare AAO thin film electrode surface.	149
Figure 4.16	(a) Bode plot and (b) Nyquist plot of the bare AAO thin film electrode, measured in a solution containing ferricyanide ions from a frequency range of 100 kHz to 10 Hz.	150
Figure 4.17	Illustration of the complete step of surface modification and DNA hybridization detection mechanism at the AAO nanoporous electrode surface.	152
Figure 4.18	(a) Bode plot and (b) Nyquist plot of AAO nanoporous electrode before and after surface modification with APTES/Glutaraldehyde, ssDNA probe immobilization and ssDNA target hybridization (10 μM).	153
Figure 4.19	EIS measurement mechanism at the cross-section of AAO nanoporous tunnels before and after surface modification on nanoporous tunnels and after the ssDNA target hybridization process.	155
Figure 4.20	Correlations effects between pore size and AAO thickness to the resistance charge transfer (R_{ct}).	159

Figure 4.21	Correlation graph of pore size and AAO thickness to the AAO thin-film electrodes sensitivity in detecting DNA hybridization.	164
Figure 4.22	Plot of SNR response versus control factor levels for the (a) sensitivity and (b) LOD, where the blue circles indicate the optimized control factor levels for the highest sensitivity (LTB) and the lowest LOD (STB), respectively.	172
Figure 4.23	The percentage influence of each control factor towards (a) the sensitivity and (b) LOD.	174
Figure 4.24	FESEM morphological images of (a) S-AAO and (b) LOD-AAO thin film electrodes at 100k magnification.	181
Figure 4.25	(a) Nyquist plot and (b) linear regression curve at five different concentrations of ssDNA target for S-AAO thin film electrode.	183
Figure 4.26	(a) Nyquist plot and (b) linear regression curve at five different concentrations of ssDNA target for LOD-AAO thin film electrode.	184
Figure 4.27	Selectivity test of S-AAO (red) and LOD-AAO (blue) thin-film electrodes after optimize the anodizing parameters using the Taguchi method.	187
Figure 4.28	Illustrations of AAO thin film electrode surfaces after each modification layer added: (a) bare, (b) silanization with APTES and glutaraldehyde, (c) immobilization of ssDNA probes and (d) DNA hybridization target.	188

LIST OF ABBREVIATIONS

AAO	Anodic aluminum oxide
AC	Alternating current
Ag/AgCl	Silver/silver chloride
Al	Aluminum
ANOM	Analysis of means
ANOVA	Analysis of variance
APTES	3-aminopropyltrimethoxysilane
ASTM	American Society for Testing and Materials
CNTs	Carbon nanotubes
CPE	Constant phase element
CV	Cyclic voltammetry
DENV2	Dengue-virus particles serotype 2
DI	Deionized water
DNA	Deoxyribonucleic acid
DOE	Design of experiment
DPV	Differential pulse voltammetry
dsDNA	Double stranded DNA
EIS	Electrochemical impedance spectroscopy
FESEM	Field emission scanning electron microscope
FFT	Fast Fourier Transform
FTIR	Fourier-transform infrared spectroscopy
GA	Glutaraldehyde
GPMS	3-glycidoxypropyl) trimethoxysilane
HA	Hard anodizing
IPA	Isopropyl alcohol
KCL	Potassium chloride
L9	Taguchi orthogonal array with 9 Lines of experimental arrays
LED	Light-emitting diode
LOD	Limit of detection
LOD-AAO	LOD optimized AAO
LTB	Larger the better
M	Molarity

MA	Mild anodizing
PBR	Pilling-Bedworth ratio
PL	Photoluminescence
PVD	Physical vapour deposition
R_{ct}	Resistance charge transfer
R_s	Solution resistance
S-AAO	Sensitivity optimized AAO
SAM	Self-assembled monolayer
SEM	Scanning electron microscopy
SNR	Signal to noise ratio
ssDNA	Single-stranded DNA
STB	Smaller the better
T	Temperature
TEM	Transmission electron microscopy
V	Voltage
W	Warburg
XRD	X-ray diffraction
XRF	X-ray fluorescence

©This item is protected by original copyright

LIST OF SYMBOLS

Al_2O_3	Aluminium oxide
Al^{3+}	Aluminum ions
Au	Aurum
$^\circ\text{C}$	Celcius
cm	Centimeter
cm^2	Centimeter square
ρ	Density
e-	Electrons
$\text{Fe}(\text{CN})_6^{3-}$	Ferrycyanide ions
Hz	Hertz
h	Hour
H_2	Hydrogen
H^+	Hydrogen ions
H_2O_2	Hydrogen peroxide
H_3O^+	Hydronium ions
-OH	Hydroxyl
L	Liter
Mn	Manganese
μ	Micro
μL	Microliter
μM	Micromolar
mA	Miliampere
mL	Mililiter
mV	Milivolts
ng	Nanogram
nm	Nanometer
nM	Nanomolar
Ω	Ohm
COO-	Oxalate
$\text{H}_2\text{C}_2\text{O}_4$	Oxalic acid
O^{2-}	Oxygen ions

O ₂	Oxygen ions
O ⁻	Oxylate
%	Percentage
H ₃ PO ₄	Phosphoric acid
π	Pi
pM	Picomolar
Pt	Platinum
ρ _p	Pore density
pH	Scale used for acidity or basic
σ	Sigma
SiO ₂	Silicone oxide
H ₂ SO ₄	Sulphuric acid
H ₂ O	Water

©This item is protected by original copyright

Sintesis Dan Pengoptimuman Elektrod Saput Nipis Aluminium Oksida Teranod Untuk Penderiaan DNA

ABSTRAK

Dalam beberapa tahun kebelakangan ini, aluminium oksida teranod (AAO) telah dieksplorasi secara meluas sebagai peranti biopenderiaan DNA yang murah, mudah alih dan sensitif. Selain dari kemampuan mereka melakukan pertumbuhan sendiri liang nano yang tersusun, keliangan yang tinggi dan keluasan permukaan yang besar, AAO mempunyai satu ciri yang sangat istimewa dimana sifat-sifat dimensinya boleh diubahsuai dan direka bentuk dengan hanya mengawal parameter utama penganodan iaitu voltan, suhu, masa dan kepekatan elektrolit. Oleh kerana kepekaan dan had pengesanan biopenderiaan AAO-DNA bergantung pada ukuran dimensi liang nano itu sendiri, maka ramai penyelidik telah berusaha untuk cuba memahami kesan bagi setiap parameter anodisasi terhadap dimensi liang nano disamping mencuba untuk mengoptimumkan dan meningkatkan kepekaan AAO dalam mengesan hibridisasi DNA. Walau bagaimanapun, kajian-kajian tersebut hanya tertumpu pada trend pemboleh ubah tunggal pada satu-satu masa dengan kaedah *one-factor-at-a-time* (OFAT), berbanding dari menyiasat semua interaksi yang mungkin di antara parameter anodisasi secara serentak. Oleh itu, mereka hanya melaporkan peningkatan terhadap kepekaan biopenderiaan AAO-DNA yang telah mereka peroleh pada julat parameter tertentu yang telah mereka uji tanpa memberikan tahap kombinasi optimum dari semua parameter anodisasi sementara parameter anodisasi yang paling kritikal dan berpengaruh masih tetap tidak diketahui. Sebagai sumbangan untuk menyelesaikan masalah ini, kaedah Taguchi telah diusulkan dalam penyelidikan ini sebagai alat pengoptimuman untuk mengkaji interaksi yang ada di antara semua parameter dan pada masa yang sama memberikan kombinasi terbaik dari semua tahap parameter untuk meningkatkan kepekaan biopenderiaan AAO-DNA pada kadar optimumnya. Sementara itu, analisis ANOVA telah dicadangkan untuk mendapatkan parameter anodisasi yang paling berpengaruh terhadap prestasi kepekaan biopenderiaan AAO-DNA. Sebelum pengoptimuman dilakukan, kajian korelasi antara dimensi liang pori dan pemindahan caj rintangan (R_{ct}) yang mempengaruhi kepekaan biopenderiaan AAO-DNA telah dilakukan. Untuk penyelidikan ini, elektrod biopenderiaan DNA saput nipis AAO akan disintesis menggunakan kaedah anodisasi langkah tunggal di dalam asid oksalik. FESEM digunakan untuk mengamati permukaan AAO, sementara EIS digunakan untuk mempelajari sistem elektrokimia bagi pengesanan hibridisasi DNA. Dari penemuan pertama, kepekaan biopenderiaan AAO-DNA didapati dipengaruhi oleh nisbah ketebalan AAO kepada ukuran liang pori. R_{ct} kekal di bawah 100 k Ω selagi nisbah ketebalan AAO kepada ukuran liang pori dikekalkan dalam julat antara 1:11 kepada 1:16. Melebihi nisbah lebih dari 1:25 akan mengakibatkan kenaikan R_{ct} secara mendadak dan mempengaruhi penurunan pada kepekaan. Dari penemuan kedua, pengoptimuman melalui kaedah Taguchi merupakan suatu pembaharuan di dalam kajian ini. Kombinasi parameter anodisasi optimum didapati pada suhu 40 V, 17°C, 0.3 M asid oksalik pada 1 jam. Pengulangan eksperimen telah dilakukan untuk mengesahkan kecekapan kaedah Taguchi di mana kepekaan elektrod biopenderiaan AAO-DNA yang telah dioptimumkan berjaya ditingkatkan kepada 62.57% pada 0.278 k Ω /M (LOD pada 6.497x10⁻¹⁵M)

berbanding dengan nominal. Dari penemuan ketiga melalui analisis ANOVA, urutan parameter anodisasi yang paling berpengaruh terhadap kepekaan AAO-DNA biopenderia adalah mengikut susunan: voltan anodisasi (34.13%) > masa anodisasi (29.85%) > suhu (20.27%) > kepekatan elektrolit (15.74%). Pada akhir penyelidikan ini, pengoptimuman sintesis elektrod sapat nipis AAO dengan kaedah Taguchi untuk penginderaan DNA telah berjaya dicapai. Oleh kerana penyelidikan ini telah menggunakan jenis DNA sasaran yang tidak spesifik bagi tujuan pembangunan prototaip, oleh itu, disasarkan bahawa elektrod sapat nipis AAO yang telah dioptimumkan sensitifnya ini akan mempunyai peluang yang lebih besar untuk digunakan secara meluas di masa depan bagi mengesan pelbagai jenis DNA seperti denggi, *E-Coli* atau *salmonella*. Diharapkan agar hasil kajian ini dapat membantu para penyelidik lain untuk mensintesis sapat nipis AAO pada tahap prestasi anodisasi optimumnya agar kepekaan biopenderia AAO-DNA dapat ditingkatkan lagi.

©This item is protected by original copyright

Synthesis and Optimization of Anodic Aluminium Oxide Thin Film Electrode for DNA Sensing

ABSTRACT

Recent years, anodic aluminum oxide (AAO) has been extensively explored as an inexpensive, portable and sensitive DNA biosensing device. Apart from their ability to self-grow into well-ordered nanoporous with high porosity and huge surface area, AAO has one special feature wherein their nanopores' dimension are capable to be altered and engineered by controlling the main anodizing parameters namely voltage, temperature, time and electrolyte concentration. Since sensitivity and limit of detection of AAO-DNA biosensor depends on the nanopores' dimension itself, therefore, many researchers have tried to understand the effect of each anodizing parameters to the nanopores' dimension while tried to optimize and improve the sensitivity of AAO in detecting DNA. However, those studies were only focused on the trend of single variable parameter at one time by one-factor-at-a-time method (OFAT), rather than investigating all the interactions between the anodizing parameters simultaneously. Hence, they only reported the improvement made to the sensitivity of their AAO-DNA biosensor at the particular parameter range that they have tested without providing the best of optimum combination levels of all anodizing parameters while the most critical and influential anodizing parameter is still remained unknown. As a contribution to solve these problems, Taguchi method has been proposed in this research as an optimization tool to study the existing interaction between the parameters while at the same time providing the best combination of all parameters levels to improve the AAO-DNA biosensor sensitivity at its optimum performance. Meantime, ANOVA analysis has been proposed to obtain the most influential anodizing parameter to the sensitivity of AAO-DNA biosensor. Prior to optimization, correlation study between the pores' dimension and resistance charge transfer (R_{ct}) that affects the sensitivity of AAO-DNA biosensor has been conducted. For this research, AAO thin film-DNA biosensor electrode was synthesized using a single step anodization method in oxalic acid. FESEM was used to observe the AAO surface, while EIS was utilised to study the electrochemical system for DNA hybridization detection. From the first finding, sensitivity of AAO-DNA biosensor was found to be influenced by the ratio of AAO thickness to the pore size. R_{ct} remained under 100 k Ω as long as the ratio of AAO thickness to the pore size was maintained in the range between 1:11 to 1:16. Exceeding the ratio of more than 1:25 will result to the sudden increased in R_{ct} and hence affecting the sensitivity to be reduced. From the second finding, optimization through Taguchi method is the main novelty of this research. The optimum combinations of anodizing parameters were found at 40 V, 17 °C, 0.3 M of oxalic acid at 1 hour. A repetition in experiment was conducted to confirm the efficiency of Taguchi where the sensitivity of the optimized AAO-DNA biosensor electrode was successfully improved to 62.57 % at 0.278 k Ω /M (LOD at 6.497×10^{-15} M) compared to the nominal. From the third finding through ANOVA analysis, the sequences of the most influential anodizing parameter to the AAO-DNA biosensor sensitivity are following the order: anodizing voltage (34.13%) > anodizing time (29.85%) > temperature (20.27%) > electrolyte concentration (15.74%). At the end of this research, optimization of the synthesis of AAO thin film electrode by Taguchi method for DNA sensing was successfully achieved. Since this

research had used nonspecific type of DNA target analytes for prototyping development purposed, therefore, it is targeted that this optimized and sensitivity improved AAO thin film electrode will have greater chance to be used widely in the future for detecting various types of DNA, such as dengue, E-coli, or salmonella. Besides, it is of great hope that the outcome from this research may help other researchers to synthesize AAO thin film at its optimum anodizing condition as to improve the sensitivity of the AAO-DNA biosensor.

©This item is protected by original copyright

CHAPTER 1 : INTRODUCTION

1.1 Background

Biosensors have emerged since a few decades ago and its application has become popular primarily in the field of food analysis, control of environmental pollution as well as in the area of human healthcare and diagnostic (Aw, et. al., 2015; Gotoh, et. al., 2014; Rothberg, et. al., 2011; Santos, Kumeria, & Losic, 2013). Since 1996, statistic shows that the world market for biosensor has been continuously increasing up to this date. Unlike conventional methods such as bio-labelled fluorescents technique that requires an extensive preparation as well as expensive label, biosensor on the other hands offers a rapid, label-free and significantly low cost measurement technique. Thus, biosensors help to improve the measurement and detection methods employed by the traditional techniques used previously.

Biosensors can be classified and named based on several criteria such as the transduction principle used (e.g. electrochemical, mass dependent or optical), the types of bio elements used as the receptor (e.g. enzyme, nucleic acid, proteins or oligonucleotides) or the types of analytes that can be detected (e.g. DNA, glucose, toxin or drugs) (Bhalla, Jolly, Formisano, & Estrela, 2016). The most basic biosensor system is usually contains of three elements, namely receptor as the sensing element, transducer as well as processor (Minaei, Saadati, Najafi, & Honari, 2015). A complete illustration on the basic of biosensor system is presented in Figure 1.1.

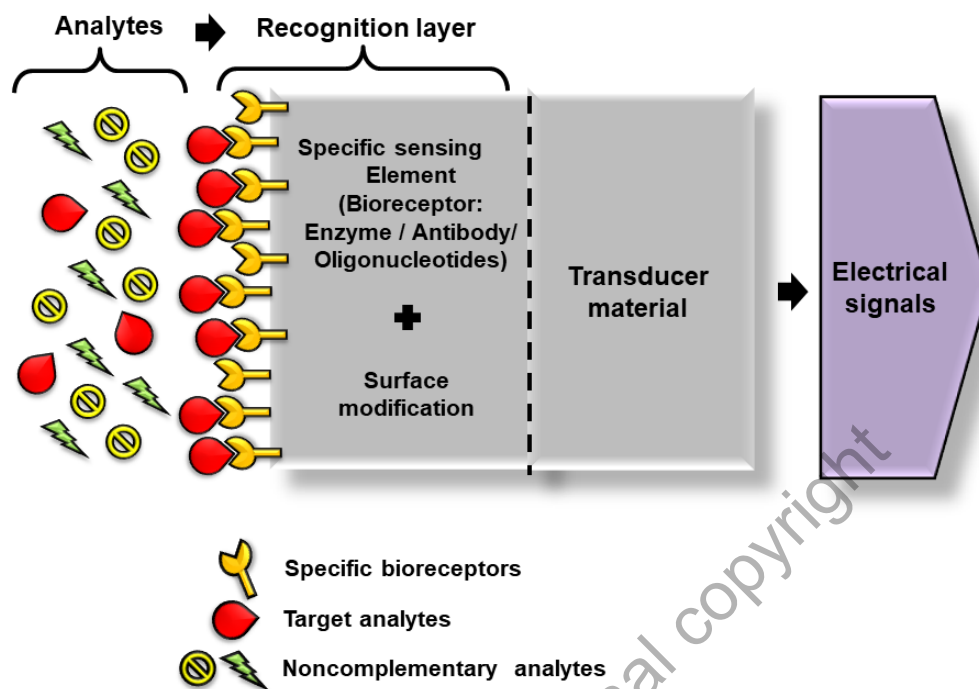


Figure 1.1 Illustration of the basic biosensor system.

Receptor is attached onto the transducer surfaces to form a recognition layer. For example, DNA biosensors use single-stranded DNA (ssDNA) probe containing 20 to 40 base pairs to be functioning as the receptor. Selected sequence of ssDNA probe is then immobilized onto the electrode surfaces by using the surface modification method. Methods that used for immobilization and surface modification are depending on the functionality properties of the electrode surface. During hybridization, receptor will selectively combine with the specific target analytes to release hydrogen ions. At the same time, the recognition layer will thicken and thus increases the resistance of the charge transfer at the transducer surfaces. Depending on the detection method used, hybridization of DNA can be detected by measuring analytical signals from the amounts of H^+ released or the changes in the resistance of the charge transfer (R_{ct}) at the transducer surfaces. These analytical signals will then receive by the transducer and converted into electrical signals to be measured. Finally, electrical signals will be